ZVS PWM BUCK-BOOST CONVERTER APPLIED TO REGENERATE THE ENERGY OF A THREE LEVEL NPC VOLTAGE-FED INVERTER WITH MODIFIED UNDELAND SNUBBER

Luiz Ricardo Lima, Marcello Mezaroba, Yales Rômulo de Novaes
University of Santa Catarina State – UDESC
89219-710, Joinville,SC - Brazil
englrlima@gmail.com, mezaroba@joinville.udesc.br, novaes@ieee.org

***Abstract* – This paper analyses the utilization of an energy regeneration circuit in a three-level NPC (Neutral-Point Clamped) voltage-fed inverter using a modified Undeland snubber. The regeneration circuit uses a QSC (Quasi-Square wave Converter) ZVS (Zero Voltage Switching) dc-dc auxiliary converter to restore the energy from the snubber capacitor to the dc bus. The regenerative circuit uses a single active switch and operates independently of the inverter. Operation stages, theoretical waveforms and a design methodology are presented. Experimental results of a 1.5 kVA prototype are included to validate the proposed topology.**

***Keywords* – NPC, Regenerative, Undeland Snubber, Multilevel Inverter**

I. INTRODUCTION

The increase in power consumption, driven by economic growth all around the world, has been a propeller for the development of solutions that increase the efficiency with which humankind consumes energy.

When approaching the problem of power conversion, some key points of development are the voltage level utilized and the commutation frequency used in high frequency static converters.[1]

The increase in the switching frequency brings a number of benefits to the converter: the reduction in the size of magnetic elements, improved control performance during transient conditions, output signal (either voltage or current) containing higher frequency components and better output signal quality. On the other hand, this frequency raise also increases electromagnetic emission and losses in switching and magnetic elements.

From the point of view of power transmission, the voltage level should be very high in order to decrease losses. Some loads also require high voltage levels. Paradoxically, the voltage limit of electronic switches decrease in switches that can be operated in higher frequencies.

The NPC (Neutral Point Clamped) inverter, proposed by Backer and Bedford [2] and later by Nabae *et al.* [3], is a solution to increase operating voltage without giving up on switching frequency. This is a solution that also permits the load to be submitted to three voltage levels or more, depending on the quantity of cells implemented. This increase in the number of voltage levels permits the elimination of harmonics and a reduction in the total harmonic distortion of the output signal as explained by Nabae.

Other solutions to allow the utilization of high commutation frequencies in high voltage applications focus on the diminution of commutation losses on the switches.

One solution widely used and studied was presented by Undeland[4]. The Undeland snubber success is due to its simplicity, good performance and robustness[5]. However, it does not increase the global efficiency of the converter, because the energy removed from the switches and stored in the storage capacitor, is posteriorly dissipated in a resistor.

In order to improve the converter efficiency, some researchers have introduced dc-dc converters to regenerate the storage capacitors energy to the input dc bus [6]-[7].

The Modified Undeland Snubber-MUS was proposed by Péres and Barbi in [8]-[9] and used by Sperb e*t al* [5] and Mezaroba *et al*[10]. These modifications allow the use of lower voltage storage capacitors. In the solution evaluated in [5] and [8] the energy is restored through a buck-boost dc-dc converter that behaves as a QSC (Quasi-Square-Wave) ZVS (Zero Voltage Switching). This topology operates with fixed and independent duty cycle, what makes its operation simple to implement. It also has a small number of components, one active switch, one inductor and one diode. The ZVS operation results in a high efficiency and low electromagnetic emission by the regenerative circuit.

A dissipative MUS was applied to a NPC 3 level inverter by Novaes and Barbi in [11]. Other snubbers have been applied to this inverter, such as Tan *et al*[12], but also with no regeneration circuit for the energy processed by the snubber. A regenerative MUS was presented by Reinert *et al* [13], but applied to a classical inverter.

This paper presents the theory and implementation of a regenerative DC-DC converter, such as in [5], applied to a NPC three-level inverter with MUS such as in [11].

This paper is organized as follows: section II explains the principle of operation of a three level NPC inverter with the MUS, section III presents the theory on the operation of the QSC-ZVS buck-boost converter, section IV shows a design methodology for the QSC-ZVS buck-boost converter. A design example, simulation and experimental results are presented in sections V, VI and VII.

II. THREE LEVEL NPC INVERTER WITH A MUS

Figure 1 shows the general scheme of the proposed topology.

The three levels NPC inverter is constituted by two NPC cells. Diode D_{g1}, switch S_1 and switch S_2 constitute the upper cell, while D_{g2}, S_3 and S_4 constitute the lower cell. In the modulation strategy chosen, the operation of S_1 and S_3 is complementary, as is operation of S_2 and S_4. The output

voltage $v_O(t)$ is positive when S_1 and S_2 are turned on, negative when S_3 and S_4 are turned on and zero when S_2 and S_3 are on. S_1 and S_4 are never turned on at the same time because $v_O(t)$ would depend on the direction of the load current and the voltage over one switch would be doubled.

One MUS for each NPC cell have to be used. Each MUS is highlighted by the dashed rectangle and is constituted by: one commutation capacitor (C_1 or C_2) that deviates energy from the switch during turn off; one inductor (L_1 or L_2) that keeps low the current through the switch while it is turned on; two diodes (D_{S1} and D_{S2} or D_{S3} and D_{S4}); and one clamping capacitor (C_{g1} or C_{g2}).

In order to evaluate the improvement in efficiency and performance that the regeneration brings to the converter, two different circuits will be used to handle the energy deviated to the clamping capacitor. The first one is the already mentioned buck-boost QSC-ZVS converter and the other one is a simple resistor that will dissipate this energy. These results will be compared to the hard switching condition.

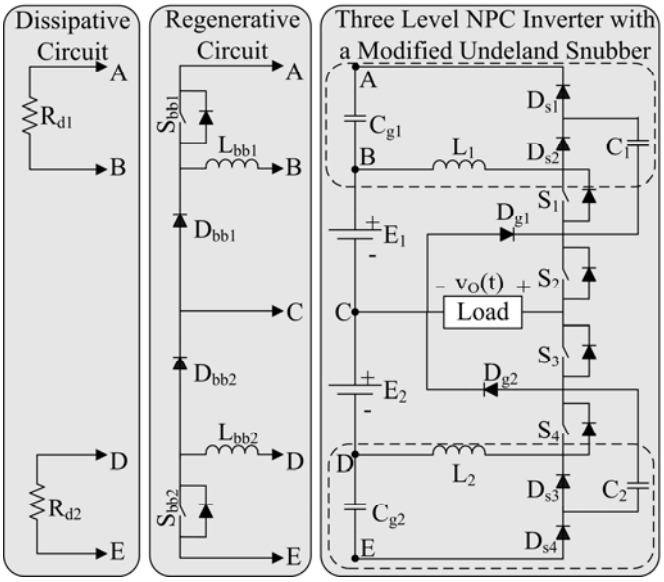

Fig. 1. Regenerative MUS applied to a three level NPC inverter.

III. REGENERATIVE CIRCUIT

Figure 2 shows the circuit that represents the QSC-ZVS buck-boost converter. In this analysis, the clamping capacitor is substituted by a dc voltage source because the voltage over this capacitor does not vary significantly in one switching period.

The diode and switch intrinsic capacitances will be represented by C_{Dbb} and C_{Sbb}, respectively. And the switch antiparallel diode is represented by D_{Sbb}. In the following analysis, the reverse recovery of diode D_{bb} will be considered because the converter uses this energy to charge the inductor L_{bb} during one interval.

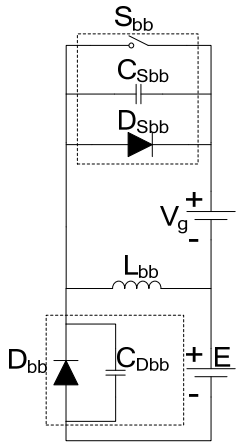

Fig. 2. QSC-ZVS buck-boost converter.

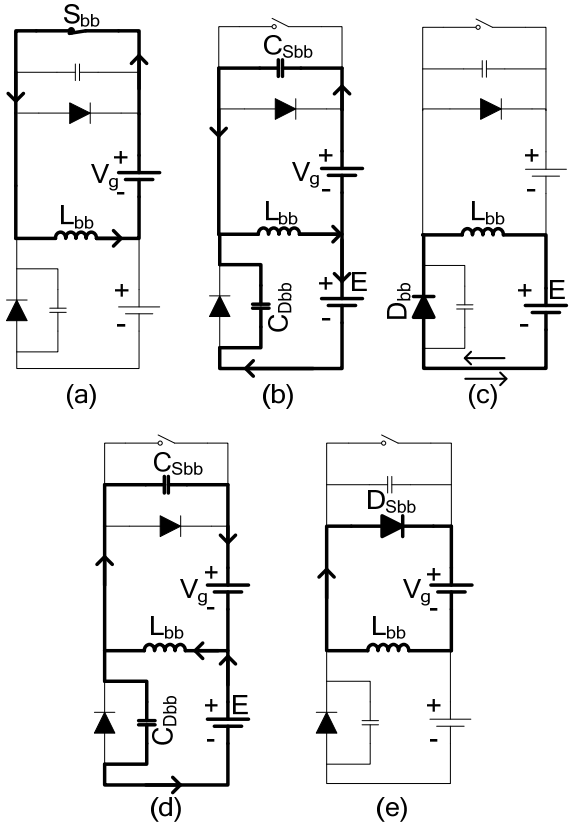

Fig. 3. Switched intervals equivalent circuits.

Five switched intervals exist in a switching period and are represented in figure 3. Each interval is described bellow:

$0 < t < t_1$: Figure 3(a) shows the equivalent circuit for this interval. It starts when the current in the inductor changes direction. The current through D_{Sbb} ceases and it starts flowing through S_{bb}. The source V_g transfers energy to the inductor L_{bb}, which has its' current linearly increased at a rate of V_g/L_{bb}.

$t_1 < t < t_2$: Figure 3(b) shows the equivalent circuit for this interval. This interval starts with the turn off of S_{bb}. The intrinsic capacitances of the switches are charged. C_{Sbb} voltage increases from 0 to V_g+E and C_{Dbb} decreases from V_g+E to 0. The inductor current is considered unchanged due the shortness of this interval.

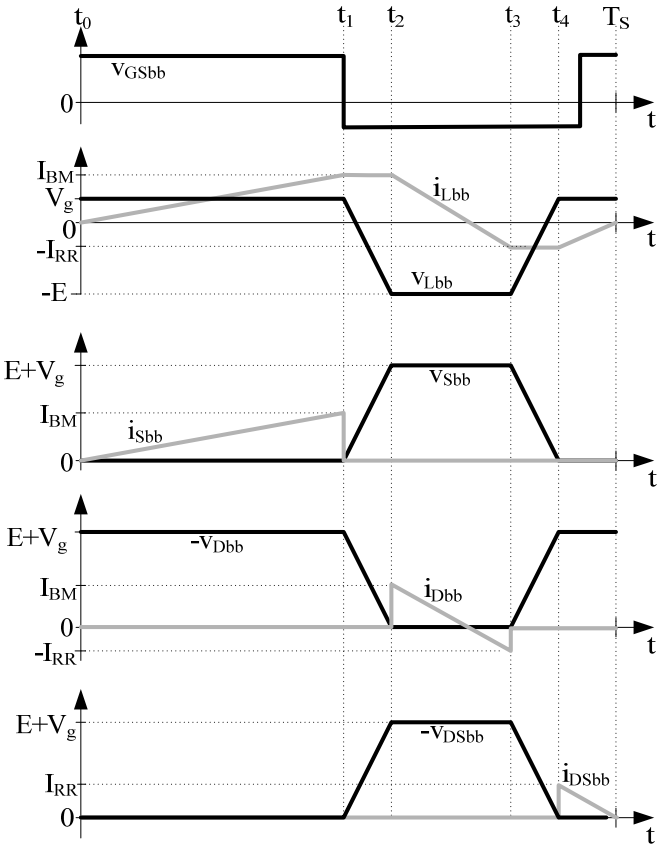

Fig. 4. QSC-ZVS buck-boost main theoretical waveforms.

$t_2 < t < t_3$: Figure 3(c) shows the equivalent circuit for this interval. It starts when the inductor current starts flowing through the diode. The current inductor decreases linearly at a rate of E/L_{bb}. When the current reaches zero, the diode reverse recovery energy is transferred to the inductor that assumes a negative current. In t_3, all this energy has been transferred. The current through the inductor reaches its maximum negative value and the diode is turned off.

$t_3 < t < t_4$: Figure 3(d) shows the equivalent circuit for this interval. The inductor current is considered unchanged due the shortness of this interval. This current flows through the switches' intrinsic capacitances. The voltage over C_{Sbb} decreases down to 0 and the one over C_{Dbb} increases up to V_g+E at t_4.

$t_4 < t < T_S$: Figure 3(e) shows the equivalent circuit for this interval. During this interval, S_{bb} must be turned on to guarantee soft commutation. In t_4, the inductor current starts circulating through D_{Sbb} and it decreases at a rate of V_g/L_{bb}. This interval ends when the current through the inductor reaches zero.

Figure 4 shows the mains waveforms for this converter.

IV. DESIGN METHODOLOGY

This section presents some guidelines to design the snubber components and the regenerative circuit.

A. Design of the Modified Undeland Snubber

Initially, one must specify some parameters for the inverter:

E – Nominal dc input voltage of each leg.

$(di_S/dt)_{max}$ – Maximum current rate of change at the switches.

$(dv_S/dt)_{max}$ – Maximum voltage rate of change over the switches.

$I_{O\text{-}pk}$ – Peak of the output current.

f_r – Low frequency of the output signal. Grid frequency, usually.

Step 1–Definition of the MUS nominal clamping voltage(V_g)

$$0.05 \cdot E \le V_g \le 0.1 \cdot E \quad (1)$$

A higher value of V_g improves the snubber functionality and the efficiency of the regeneration converter, but it also increases the overvoltage applied to many components in the circuit. The range above is usually used.

Step 2-Determinantion of the snubber inductance L that limits the current rate of change of the main switches:

$$L = \frac{V_g}{\left(di_S / dt\right)_{\max}} \quad (2)$$

Step 3-Determination of the snubber capacitance C that limits the voltage rate of change of the main switches:

$$C = \frac{I_{O-pk}}{\left(dV_S / dt\right)_{\max}} \quad (3)$$

Step 4-Simulation to adjust C and L values and to estimate the power processed from the switching losses (P_g).

The addition of the snubber circuit brings some alterations to the inverter functioning. Some over currents appear and the analytical computation of power losses in the switches and the power processed by the snubber are extremely complex. Simulation tools are the solution to this stage of the design.

Some key points are important during this step:

- C_g can be replaced by a dc voltage source V_g in order to simplify analysis and decrease simulation time.
- The semiconductor models should be accurate and obtained from the manufacturer.
- The simulation should last at least one low frequency period because the power processed by the snubber is not the same in all switching periods.

Step 5-Determination of the clamping capacitor value.

$$C_g = \frac{P_g}{2\Delta V_g \cdot f_r \cdot V_g} \quad (4)$$

Each snubber only operates during half of the low frequency period. Because of this, C_g must be big enough to maintain its voltage high during this half period. The size of this capacitor can be diminished by disabling the circuit connected to withdraw the energy from C_g, either R_d or the regenerative converter. It is important to point that the minimum size of C_g is also delimited by its series resistance.

Resistor R_d, showed in figure 1, is connected in parallel with capacitor C_g to dissipate the energy stored by it. This resistance can be calculated by:

$$R_d = \frac{V_g^2}{P_g} \quad (5)$$

B. Regenerative Converter Design

When using the regenerative converter, resistor Rd is removed from the circuit. This design methodology was based on the one proposed by [9]. Initially, the commutation frequency of the buck-boost converter (f_{Sbb}) should be stipulated. Power processed by the converter (P_g), input voltage (V_{dc}) and output voltage (E) should already be known from the snubber design. Using this information, the following steps are followed to project the converter:

Step 1 – Diode selection: it should support a voltage stress of $E+V_g$ and an average current of:

$$I_{Dbb-avg} = \frac{P_g}{V_{dc}} \tag{6}$$

From the diode datasheet, its junction capacitance (C_{Dbb}), reverse recovery time (t_{rr}) and reverser recovery charge (Q_{rr}) can be obtained. With these values, the peak recovery current can be calculated:

$$I_{rr} = 2 \cdot \frac{Q_{rr}}{t_{rr}} \tag{7}$$

Step 2 – Determination of the nominal duty-cycle:

$$D_{nom} = \frac{E}{E + V_g} \tag{8}$$

Step 3 – Determination of the inductor:

$$L_{bb} = \left(a - \sqrt{a^2 - b}\right) \cdot E \cdot \left(1 - D_{nom}\right)^2 \tag{9}$$

Where:

$$a = \frac{1}{2 \cdot f_{Sbb} \cdot I_{Dbb-avg}} + \frac{4 \cdot Q_{rr}}{6 \cdot I_{Dbb-avg}^2} \tag{10}$$

$$b = \frac{1}{\left(2 \cdot f_{Sbb} \cdot I_{Dbb-avg}\right)^2} \tag{11}$$

The maximum current through the inductor is given by:

$$I_{Lbb-pk} = \frac{D_{nom} \cdot V_g}{f_{sbb} \cdot L_{bb}} - I_{rr} \tag{12}$$

Knowing the values of L_{bb} and of the peak current through it, the diode rms current can be calculated:

$$I_{Dbb-rms} = \sqrt{\frac{L_{bb} \cdot f_{Sbb} \cdot \left(I_{rr}^3 - I_{Lbb-pk}^3\right)}{3 \cdot E}} \tag{13}$$

Step 4 – Definition of the switch S_{bb} that support a voltage peak of $E+V_g$ and an average current of:

$$I_{Sbb-avg} = \frac{f_{sbb} \cdot V_g \cdot t_{sw}^2}{2 \cdot L_{bb}} \tag{14}$$

Where:

$$t_{sw} = \frac{D_{nom}}{L_{bb}} - \frac{I_{rr} \cdot L_{bb}}{V_g} \tag{15}$$

The output capacitance of the selected switch (C_{Sbb}) can be obtained from its datasheet.

The rms current through the switch is given by:

$$I_{Sbb-rms} = \frac{V_g}{L_{bb}} \cdot \sqrt{\frac{t_{sw}^3 \cdot f_{Sbb}}{3}} \tag{16}$$

Step 5 – Verification of the soft-commutation condition:

$$Q_{rr} > \frac{3 \cdot \left(C_{Sbb} + C_{Dbb}\right) \cdot \left(E + V_g\right)^2}{4 \cdot E} \tag{17}$$

If this condition is not met, the regenerative circuit does not operate with ZVS and the converter will be less efficient. In order to make the converter operate with ZVS, it is necessary to choose another diode with a greater reverse recovery time and repeat all the steps of the design.

Also in order to accomplish zero voltage commutation, the duty ratio D should be within the following interval:

$$D_{min} < D < D_{nom} \tag{18}$$

Where D_{min} is the duty cycle that would make the turn on command coincide with t_4 and can be calculated by:

$$D_{min} = D_{nom} - \frac{2 f_{Sbb}}{V_g} \cdot \sqrt{\frac{L_{bb} \cdot E \cdot Q_{rr}}{3}} \tag{19}$$

V. DESIGN EXAMPLE

This section presents a design example of the proposed inverter, snubber and regenerative circuit.

Table 1 presents the three level inverter main specifications. Table 2 presents some specification chosen, based on table 1, to design the snubber using methodology presented in section IV-A. The snubber parameters resultant from this methodology is presented in table 3.

Table 4 contains the switches and diodes characteristics, which are necessary to design the QSC-ZVS buck-boost converter, as presented in section IV.B. The last table displays the results of the regenerative converter design.

TABLE 1
Inverter Specifications

E = 400V	Nominal half DC bus voltage
$V_{O\text{-}max}$ = 220 Vrms	Output phase to neutral voltage
$V_{O\text{-}min}$ = 127 Vrms	Output phase to neutral voltage
P_O = 1.5kVa	Output power
$f_S = f_{Sbb}$=200kHz	Switching frequency of the main and regenerative converters
L_O = 560µH	Output filter inductance
C_O = 4.4µF	Output filter capacitance
IRGP50B60PD1	Switches of the main and regenerative converters
HFA15TB60	Diodes of the main and regenerative converters

TABLE 2
Snubber Specifications

di_S/dt_{MAX} = 200 A/µs	Maximum rate of current change
dv_S/dt_{MAX} = 4 V/ns	Maximum rate of voltage change
$I_{O\text{-}pk}$ = 16.97A	Output peak current
ΔV_g = 20%	Maximum voltage ripple across the clamping capacitor

TABLE 3
Main Components of Modified Undeland Snubber

V_g = 40V	Nominal clamping voltage
P_g = 75W	Power transferred to C_g
L = 5µH	Snubber inductance
C = 4.7nF	Snubber capacitance
C_g = 1.86mF	Snubber clamping capacitor

TABLE 4
Specifications of D_{bb} and S_{bb}

t_{rr} = 80ns	Reverse recovery time of D_{bb}
Q_{rr} = 50nC	Reverse recovery charge of D_{bb}
di_d/dt_{MAX} = 35A/µs	Maximum rate of change of reverse recovery current in D_{bb}
C_{Dbb} = 34pF	Junction capacitance of D_{bb}
C_{Sbb} = 100pF	Output capacitance of S_{bb}

TABLE 5
QSC-ZVS buck-boost parameters

D_{nom} = 0.909	Nominal duty-cycle
D_{min} = 0.798	Minimum duty-cycle
L_{bb} = 18.5µH	Buck-boost inductance
$I_{Lbb\text{-}pk}$ = 8.57A	Maximum current through L_{bb}
$I_{Dbb\text{-}avg}$ = 0.36A	Average current through D_{bb}
$I_{Dbb\text{-}rms}$ = 1.40A	RMS current through D_{bb}
$I_{Sbb\text{-}avg}$ = 3.40A	Average current through S_{bb}
$I_{Sbb\text{-}rms}$ = 4.41A	RMS current through S_{bb}

VI. SIMULATION RESULTS

In this section, simulation results of the regenerative circuit and of the effect of the snubber on the commutation of the main switches are presented. Both simulations were done with software Orcad Pspice 16.

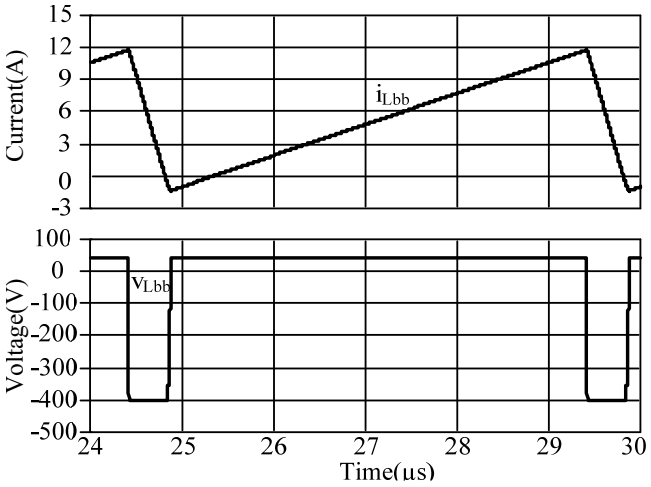

Fig. 5. Current and voltage waveforms of the buck-boost inductor.

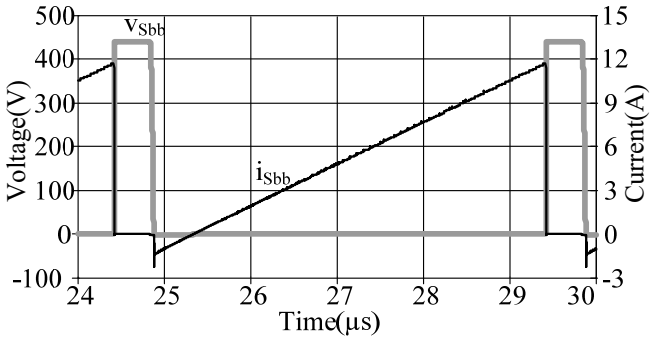

Fig. 6. Collector-emitter voltage and current waveforms of the auxiliary switch S_{bb}.

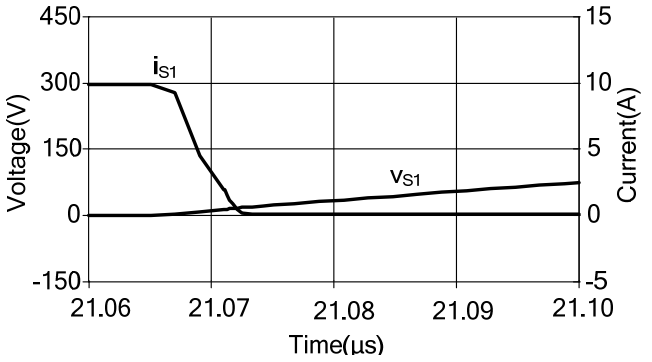

Fig. 7. Current and collector-emitter voltage waveforms of the main switch S_1 during turn off with snubber.

Figure 5 shows the voltage and current waveforms of inductor L_{bb}. Figure 6 presents the collector-emitter voltage of the auxiliary switch S_{bb}. It is possible to observe that this switch commutates under zero voltage, minimizing commutation losses.

Figures 7 to 10 show the current and voltage of the main switches during turn on and turn off, with and without the projected snubber.

Comparing figures 7 and 8, one can observe that commutation losses are reduced by decreasing the voltage rate of change during the turn off of the switch, while the current decreases to zero quickly.

The improvement in turn on is not so obvious. But figures 9 and 10 show that, with the snubber, the voltage-current cross occur at a substantially lower voltage and the current reaches its maximum value sometime after the voltage has reached zero.

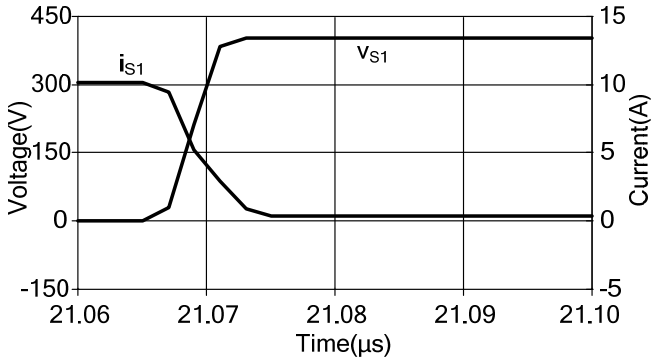

Fig. 8 . Current and collector-emitter voltage waveforms of the main switch S_1 during turn off without snubber.

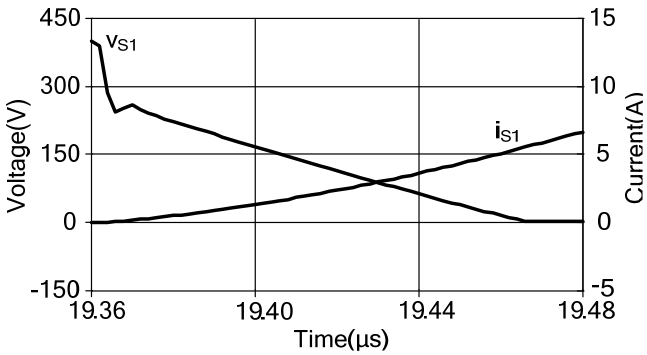

Fig. 9. Current and collector-emitter voltage waveforms of the mains switch S_1 during turn on with snubber.

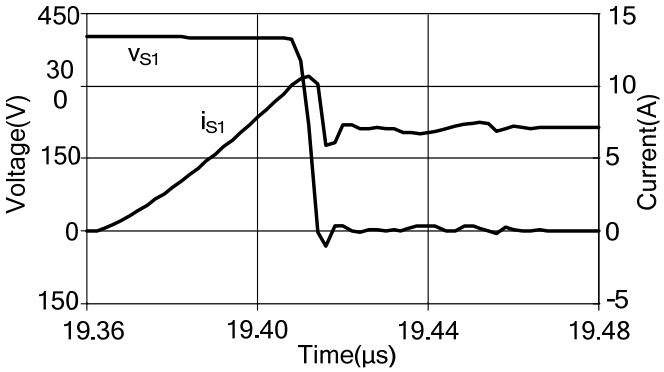

Fig. 10. Current and collector-emitter voltage waveforms of the main switch S_1 during turn-on without snubber.

VII. EXPERIMENTAL RESULTS

Based on the project presented on section V, a prototype was implemented. Figures 11 to 15 show current and voltage waveforms of a few components of the NPC inverter and of the regenerative Buck-Boost Converter.

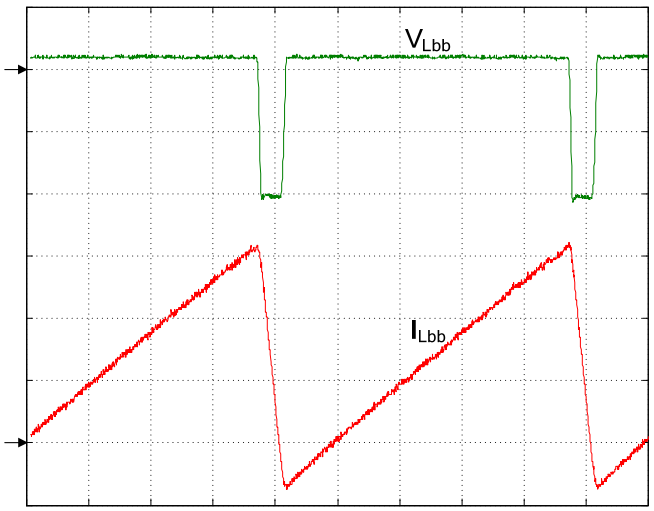

Fig. 11. Current and voltage waveforms of the buck-boost inductor L_{bb} (2,5A/div, 200V/div, 1µs/div)

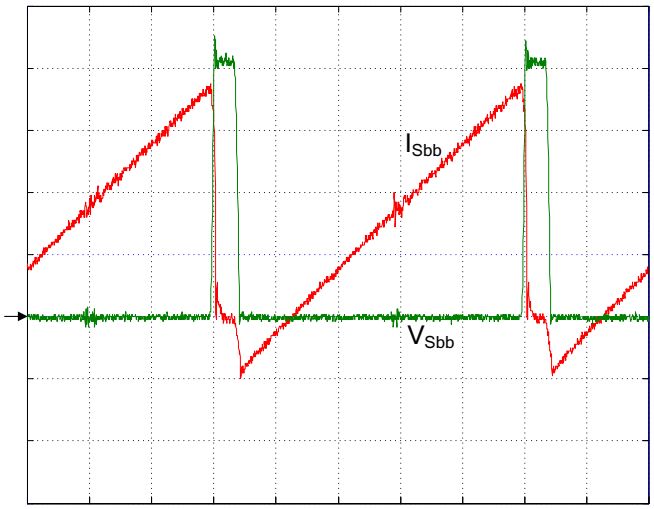

Fig. 12. Current and voltage waveforms of the auxiliary switch S_{bb} (2A/div, 100V/div, 1µs/div)

Figure 11 shows current and voltage over the buck-boost inductor.

Figure 12 presents current and voltage over the auxiliary switch S_{bb}. It can be noticed that, when current becomes positive, the voltage over this switch is zero, characterizing ZVS.

Figure 13 shows the results of voltage and current over main switch S_1. There is a very high frequency oscillation in both, current and voltage. This oscillation is probably due an interaction of the snubber elements with circuit parasitic inductances and semiconductors intrinsic capacitances. The over-current through the switch reaches 100% of the load current.

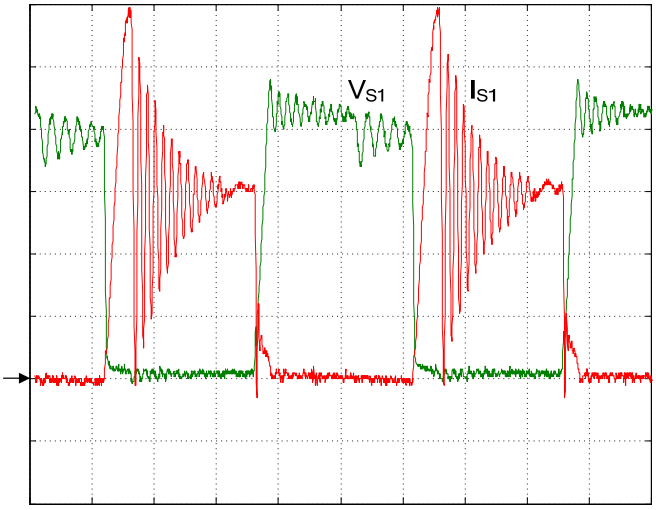

Fig. 13 Current and collector-emitter voltage waveforms of the main switch S_1 with snubber (2A/div, 100V/div, 1µs/div)

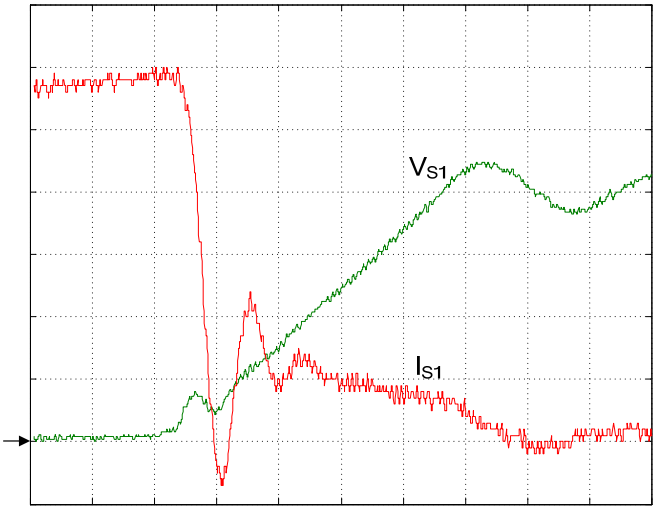

Fig. 14.Current and voltage waveforms of the main switch S_1 during turn off with snubber. (2A/div, 100V/div, 50ns/div)

Figures 14 and 15 show S_1 commutation details. Figure 14 presents the turn off. It can be noticed that the current first drop happens at quite low voltage. Majority of the commutation losses, in this case, are due the IGBT tail current.

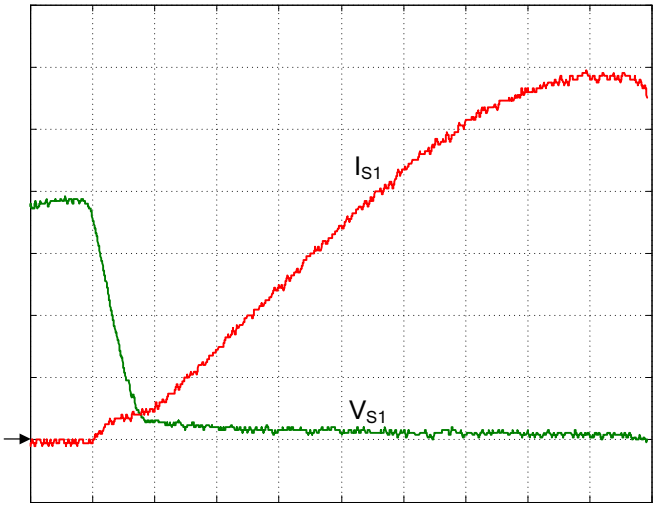

Fig. 15. Current and voltage waveforms of the main switch S_1 during turn on with snubber (4A/div, 100V/div, 50ns/div)

Figure 15 shows the turn on of S_1. It can be seen that voltage drops to nearly zero with very low current over the semiconductor. Current starts rising significantly, only after the voltage has dropped to a very low level.

Figure 16 presents output current and voltage for the inverter operating with an inductive load.

Figure 17 presents the prototype efficiency results for an output voltage of 127Vrms. The X axis presents the percentage of the nominal power. It can be seen that when operating above 80% of the nominal load, the inverter with regenerative snubber becomes more efficient than the operation with no snubber.

The operation with dissipative snubber has much lower efficiency than the other two configurations. Its' use is recommended only when efficiency is not a major concern.

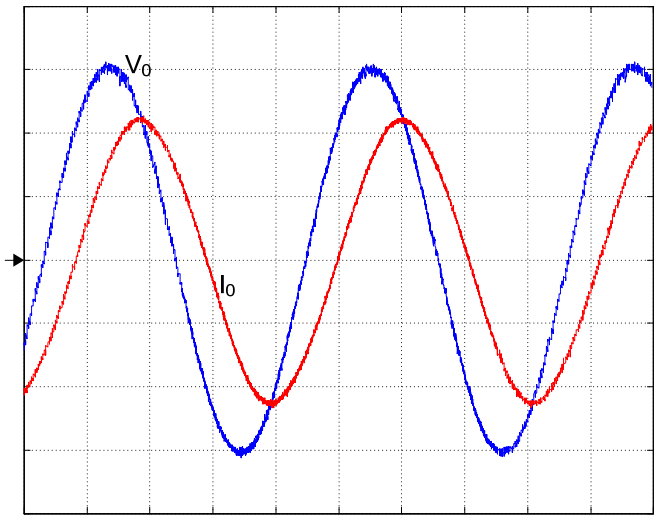

Fig. 16 – Output current and voltage (2A/div, 100V/div, 4ms/div)

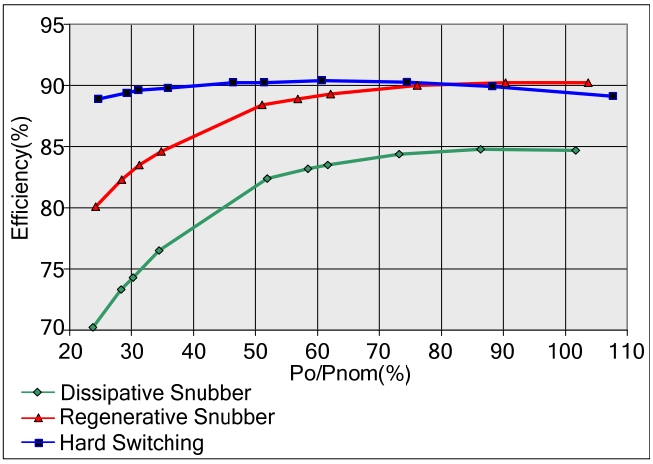

Fig. 17. Efficiency results comparison for 127Vrms output voltage

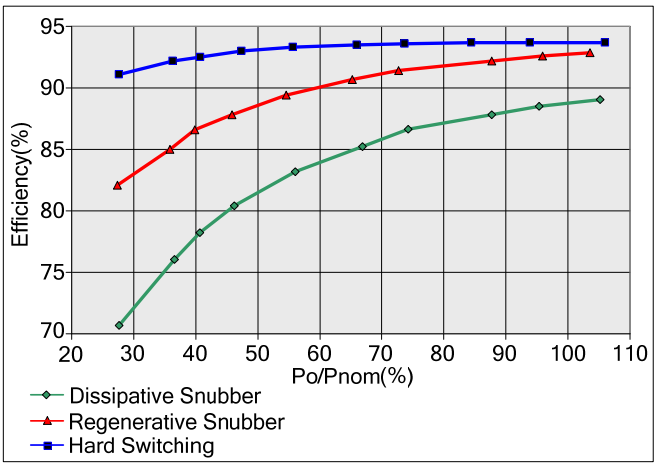

Fig. 18. Efficiency results comparison for 220Vrms output voltage

Figure 18 presents the same results for an output voltage of 220Vrms. Efficiency levels of all three curves are shifted up 1% to 4%. In these conditions, the operation with regenerative snubber never is as efficient as the operation without snubber. However, because the efficiency is higher and current levels are lower, it seems possible for the inverter to operate at powers above the one tested. In these over-power conditions, the regenerative snubber curve shows a tendency to overcome the hard switching operation curve.

VIII. CONCLUSION

Project methodology and simulation were verified by prototype implementation. A major difference in experimental results was the oscillation of the main switch current. Other experimental waveforms presented values very close to the theoretic and simulation equivalents.

The analyzed snubber was efficient in removing energy losses from the main switches of the inverter, presented an easy design method and a reasonable number of components.

The regenerative circuit proved to operate properly and independently of the main converter, improving its overall efficiency when operating near nominal load and with 127Vrms output voltage. In terms of efficiency, the use of this regenerative snubber is recommended only when the inverter operates most of the time with high load, otherwise, the operation without snubber is more efficient.

The overall efficiency improvement allows a diminution in the heat sink size. The utilization of the snubber results in lesser EMI emission, decreasing the necessity of EMI filters and reducing these filters size when they are needed.

ACKNOWLEDGEMENT

The development of this project received support from the University of Santa Catarina State (UDESC) and from the National Council of Scientific and Technological Development (CNPq), Brazil.

REFERENCES

[1] Y. R. de Novaes, “Estudo de um Snubber para o Inversor de Três Níveis com Neutro Grampeado”. *Dissertação de Mestrado*. INEP/UFSC – 2000.

[2] R. H. Backer, M. Bedford, “Bridge Converter Circuit”, *United States patent 4270163*, 1979.

[3] A. Nabae, I. Takahashi, H. Akagi, “A New Neutral-Point-Clamped PWM Inverter”, *IEEE Transactions on Industry Applications*, vol. IA-17, no. 5, pp. 518-523, September/October 1981.

[4] T. Undeland, “Switching Stress Reduction in Power Transistor Converters”, 1976.

[5] J. D. Sperb, I. X. Zanatta, L. Michels, C. Rech, M. Mezaroba, “Regenerative Undeland Snubber using a ZVS PWM DC-DC Auxiliary Converter applied to Three-Phase Voltage-Fed Inverters*”, IEEE Transactions on Industrial Electronics*, 2010.

[6] J. A. Taufiq, "Advanced inverter drives for traction," *Fifth European Conference on in Power Electronics and Applications,* pp. 224-228 vol.5, 1993.

[7] P. M. Swanepoel, J. D. van Wyk, "The effect of the regenerative Undeland snubber circuit on inverter loads", *Conference Record of the 1992 IEEE in Industry Applications Society Annual Meeting*, pp. 872-879 vol.1, 1992.

[8] A. Peres, I. Barbi, "Experimental results of the new ZVS PWM voltage source inverter with active voltage clamping and comparison with classical structure,", Telecommunications Energy Conference, 2000. INTELEC. Twenty-second International, 2000, pp. 173-179.

[9] A. Péres, "*Uma Nova Família de Inversores com Comutação Suave Empregando a Técnica de Grampeamento Ativo*" PHD, DEE, Federal University Santa Catarina, Florianópolis SC Brazil, 2000.

[10] M. Mezaroba, A. L. Batschauer, J. A. Heerdt, "Conversor CC-CA para Amplificação de Formas de Onda Genéricas Empregando Snubber Regenerativo," *5th IEEE/IAS International Conference on Industry Applications*, Salvador BA, Brazil, 2006.

[11] Y. R. de Novaes, I. Barbi, “Analysis, Design And Experimentation Of A Snubber For The Three-Level Neutral Clamped Inverter”, *Brazilian Power Electronics Conference,* pp. 577-582, COBEP 2001.

[12] T. Tan; K. Jiang; Q. Jiang; G.; Y. Lai; , “An improved McMurry snubber for Three-level NPC IGBT converter*”, International Power Engineering Conference*. , vol., no., pp.666-671, 3-6 Dec. 2007.

[13] M.R. Reinert, C. Rech, M. Mezaroba, L. Michels, "Transformerless double-conversion UPS using a regenerative snubber circuit" *Brazilian Power Electronics Conference*, pp.564-570, Sept. 27 2009-Oct. 1 2009.